p-ISSN 2089 – 0133 e-ISSN 2477-6416
URL : https://jurnal.uns.ac.id/ijap/article/view/76028
Indonesian Journal of Applied Physics (IJAP) Vol. 13 No. 2 page 276
DOI : https://doi.org/10.13057/ijap.v13i2.76028

LOW-TEMPERATURE CALCINATION OF TiO_2 AND ZnO PARTICLE FILM AND EVALUATION OF THEIR PHOTOCATALYTIC ACTIVITY

Inovasari Islami[1], Lutfi Naufal Ramadhika[1], Lusi Safriani[2], Ayi Bahtiar[2], Fitrilawati[2], Nowo Riveli[2], Annisa Aprilia*[2]

[1]Magister Physics Study Program, Universitas Padjadjaran, Bandung, Indonesia
[2]Department Physics, Universitas Padjadjaran, Bandung, Indonesia
*a.aprilia@phys.unpad.ac.id

Received 07-05-2023, Revised 21-08-2023, Accepted 24-09-2023
Available Online 24-09-2023, Published Regularly October 2023

ABSTRACT

In this study, TiO_2, ZnO, and TiO_2/ZnO films were prepared under low calcination temperature and characterized to observe their properties related to photocatalytic performance. The samples were prepared by mixing the gel phase of ZnO precursor, TiO_2 anatase powder, triton-x 100, and acetylacetone to produce a paste form for the deposition process. The resulting paste was then deposited by screen printing onto a glass substrate and subjected to calcination at 150°C to facilitate the ZnO crystallization and remove other additive materials. XRD analysis confirms that the formation of ZnO and TiO_2 crystals was assisted, although their crystallinity was lower than corresponding particulate forms. The lower crystallinity seems to be related by additive materials remains. The surface morphology of each sample was observed by scanning electron microscopy (SEM) imaging, Brunauer–Emmett–Teller (BET), and contact angle examination. Interestingly, both TiO_2 and ZnO layers tend to have a hydrophobic surface; meanwhile, TiO_2/ZnO has a hydrophilic surface. BET analysis revealed that ZnO has the highest specific surface area due to a nanosized. FTIR spectra confirmed the presence of appropriate chemical bonds in the ZnO and TiO_2 and other additive materials, such as alkyl groups. The photoluminescence (PL) spectrum shows a blue emission associated with intrinsic defects, such as vacancies and interstitials of Zn and Ti in all samples. Differences in the photocatalytic performance of film and particulate form for each material were observed and analyzed. All samples' structures, morphology, and PL characteristics were then correlated to their photocatalyst behaviour for methylene blue degradation.

Keywords: screen printing; sol-gel method; films; hydrophobic surface; ZnO particle; TiO_2; photocatalyst; adsorption; methylene blue

Cite this as: Islami, I., Ramadhika, L. N., Safriani, L., Bahtiar, A., Fitrilawati., Riveli, N., & Aprilia, A. 2023. Low-Temperature Calcination of TiO_2 and ZnO Particle Film and Evaluation of Their Photocatalytic Activity. *IJAP: Indonesian Journal of Applied Science*, *13*(2), 276-288. doi: https://doi.org/10.13057/ijap.v13i2.76028

INTRODUCTION

Titanium dioxide (TiO_2) and zinc oxide (ZnO) are two famous materials in a photocatalyst[1]. These two metal oxides have a similar band gap of around 3.2 ~ 3.3 eV, n-type semiconductor, non-toxic, biocompatible, high physical-chemical stability, and high photosensitivity[2-3]. The coupling between TiO_2 and ZnO has been reported can increase the photocatalytic performance due to enhancement in chemical activity such as redox reaction, wider absorption of the electromagnetic spectrum, and reduction of charge recombination[4]. According to the research conducted by Hellen et al., ZnO/TiO_2 composite has better optical absorption properties than pure ZnO and TiO_2[5]. Amananti et al., 2016 prepared the TiO_2/ZnO layers using the sol-gel

spray coating method, and showed better photocatalytic performance compared to individual materials caused by decreased energy band gaps and the combination of the two can modify electron and hole processes[6]. The ratio composition of TiO_2 and ZnO in composite form also influences photocatalyst behavior. Zinc concentration in the composite has been reported can affect the material phase, band-gap value, and visible light activity[7]. An optimal composition in TiO_2-ZnO heterojunction can improve the surface area and interfacial charge transport thus, the charge recombination was reduced[8]. The same results in our previous research show that the ZnO/TiO_2 composite performs better in degrading 3 ppm of methylene blue (MB) at the first 20 minutes compared to its individual usages. The combination between ZnO and TiO_2 enhances the generating charge carrier and charge transport since faster MB degradation was observed[1].

Many studies have synthesized the TiO_2-ZnO composite using several techniques such as thermal decomposition of salts, sol-gel, pyrolysis spray, hydrothermal, coprecipitation, electrospinning, and solid-state reaction[1, 9-13]. The behavior and functionality of materials obviously depend on the synthesis and preparation method used. The structure and morphology of the composite affect the ability to produce free charge carriers to assist hydroxyl radical formation. The generated hydroxyl radicals (OH·) are strong oxidants to oxidize the organic compounds[8]. In a photocatalytic system, the nanostructure of the catalyst, even in particulate or film form, shows a different performance. Nanoparticles/nanoparticles can be easily suspended in a solution but also easily agglomerates which contributes to reducing effective surface area and have an issue in catalyst removal. Meanwhile, although the nanofilms/layers have a lower effective surface area, the post-treatment to remove the catalyst in the system is not required[14]. In addition, the catalyst film can be deposited on a certain substrate and offer a reusable ability.

The photoactivity of a photocatalyst is affected by the ability to absorb incoming photons by material surfaces. Thus, nanoparticulate catalyst shows an outstanding performance owing to their large surface area compared to nanofilm[15]. Moreover, particle size seems dominantly influence the photocatalytic activity rather than crystallinity for the same systems photocatalyst. The important role in photocatalyst systems is producing free charge carriers (electron and hole) rather than interparticle charge transport due to the advanced oxidation process[16]. According to our previous research, low-temperature calcination (at 150°C) of ZnO-gel precursor (which is produced by the same route) has produced an excellent ZnO nanocrystal as a photocatalyst material[1]. In order to maintain the original properties of ZnO as produced at 150°C, we prepared TiO_2/ZnO hetero-particle film by screen printing technique and subsequently calcinated at low temperature (250°C) to remove the solvent and other additive materials.

METHOD

The synthesis of the ZnO-gel precursor was carried out by the sol-gel method that refer to our previous research[1]. The typical experimental procedure for synthesizing ZnO-gel precursor is presented as follows. One gram of zinc acetate dihydrate ($Zn(CH_3COO)_2.H_2O$) was dissolved in 42 mL of methanol in a three-neck bottle and was stirred on a magnetic stirrer for 10 minutes at 65°C using a reflux system. 0.28 grams of NaOH was dissolved in 23 mL of methanol using an ultrasonic bath until a homogeneous solution was achieved. The NaOH solution and $Zn(CH_3COO)_2.H_2O$ solution (after refluxing for ±30 minutes) were mixed and were continued refluxing for ±90 minutes until the colour change of solution was observed (from white to

transparent and return to milky white). After obtaining a milky white solution, the solution was precipitated for at least 48 hours. The gel-precipitate was collected into a centrifugation tube and methanol and hexane (1:1) were added for washing treatment. The solution was centrifuged at 3600 rpm for 10 minutes with three repetitions to obtain the ZnO-gel precursor. The ZnO gel precursor was annealed at 150°C in a vacuum oven for 8 hours to obtain ZnO in particulate forms.

The composite paste was prepared by mixing the 0.15 gram ZnO-gel precursor with 0.06 gram of TiO_2 anatase powder (i-chemical). Three drops of methanol were dropped and were blended using a magnetic stirrer until both materials were homogeneous, and subsequently were annealed at 150°C in a vacuum oven for 8 hours. Acetylacetone, triton-X, and DI water were added to the mixture of TiO_2/ZnO powdered and blended manually until a paste formed. ZnO and TiO_2 individual pastes were also prepared using the same method. The screen-printing method was used to fabricate all samples in film form. The Glass substrate was cleaned before use and continued by screen printed the paste onto it. Next step, the film was heated using a hot plate at 180°C for 8 hours and increased moderately to 250°C for 4 hours. ZnO and TiO_2 film was also prepared using ZnO and TiO_2 pastes in the same route. All sample films look homogeneous, without cracks, and not easily peeled off (Figure 1).

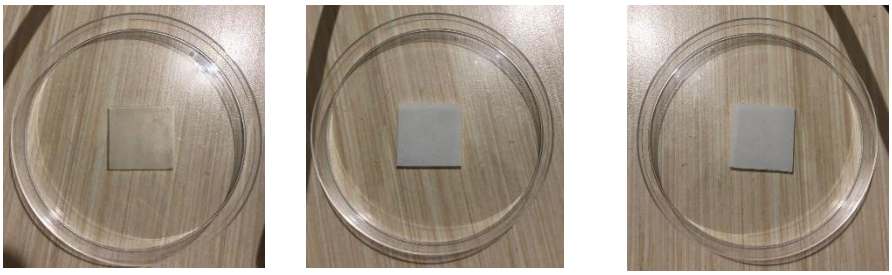

(a) (b) (c)

Figure 1. All sample film results (a) ZnO, (b) TiO_2, and (c) TiO_2/ZnO

All sample films were then subjected to various characterizations to investigate their crystal structure, morphology, compound composition, surface properties, and optical properties. The characterization includes XRD (X-ray diffraction) analysis, SEM (Scanning Electron Microscopy) imaging, EDS (Energy-Dispersive X-ray Spectroscopy) elemental analysis, Contact Angle measurement, Photoluminescence analysis, BET (Brunauer Emmett Teller) analysis for surface area determination, and FTIR (Fourier-transform infrared spectroscopy) analysis to identify the chemical bonds and functional groups present in the film. The evaluation of photocatalytic activity was examined using methylene blue solution under UV-A light irradiation. The catalyst film (surface area of film = 36,5 x 10^{-4} m) was immersed in the test solution in dark conditions under stirring for 24 hours for sample pretreatment. The photocatalytic test was taken in 4-hour irradiation with 60-minute intervals under UV-A irradiation.

RESULT AND DISCUSSION

XRD (X-Ray Diffraction) Characterization

The XRD patterns for all sample films are shown in Figure 2(a). The XRD pattern shows that the ZnO film has a hexagonal wurtzite structure that agrees with COD No. Data. 00-230-0450

and the TiO_2 film was confirmed as TiO_2 anatase phase corresponds to COD 00-500-0223. In the ZnO/TiO_2 hetero-particle film, the spectrum is only present for the TiO_2 anatase phase, while ZnO peaks are unidentified. This situation probably occurs caused by a smaller crystallite size of ZnO particles compared to TiO_2. Based on the calculation of the degree of crystallinity (DOC), which is tabulated in Table 1, but the individual ZnO and TiO_2 films do not have significant differences. ZnO film appears to consist of smaller nanoparticles/nanocrystals, thus exhibiting amorphous characteristics when mixed with TiO_2. Different results are obtained in particulate form, although the samples only calcinate at 150°C (Figure 2(b)). The degree of crystallinity (DOC) and crystallite size is significantly decreased from particulate to the layer/film form of 74.39% to 26.49% for ZnO, 80.5% to 24. 59% for TiO_2, and 73.13% to 16.6% for TiO_2/ZnO. The crystallite size of all samples is calculated using the Debye-Scherrer equation.

In the preparation of the TiO_2/ZnO particulate sample, the ZnO-gel precursor was mixed with TiO_2 anatase powder, subsequently to the annealing process. The formation of ZnO crystal is affected by the TiO_2 anatase powder. Considering the ZnO-gel precursor is rich in oxygen and hydroxyl group, the chemical reaction of TiO_2 and such group is possible to occur, leading to increasing TiO_2 crystallite size [1]. The crystalline structure of the fabricated layer tends towards an amorphous phase because of the reaction between the particles and the solvent/surfactant, which can change the surface chemical bonds and crystal quality during the heating process[17]. The reduction crystallite size of TiO_2 (48.66 nm in individual TiO_2 film to 39.35 nm in TiO_2/ZnO film) was attributed to the presence of ZnO compounds and surfactant in the paste preparation step. The surface reactions between oxygen on TiO_2 and ZnO with organic compounds from surfactant and solvent can increase the amorphous phase inside the film. The existence of amorphous phase can deteriorate the XRD spectrum (broadening in FWHM) [18]. In fact, the amorphous phase can be suppressed by further heating process (more than 250°C)[19-20]. The ZnO crystallite size in individual film is 5.69 nm, whereas in the ZnO/TiO_2 film, the ZnO crystallite size was uncalculated due to the peak of ZnO in XRD spectrum is not observed. The DOC and crystallite size of each sample are tabulated in Table 1.

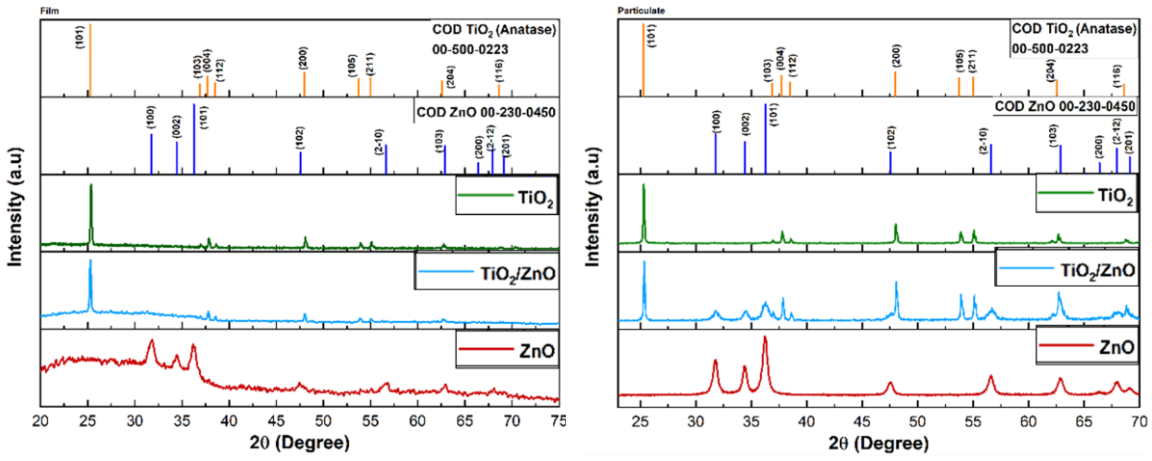

(a) (b)

Figure 2. XRD patterns of all samples (a) film, (b) particulate form

Table 1. Calculation of the Degree of Crystallinity (DOC) and crystallite size of the catalyst material

Material	DOC (Degree of Crystallinity)		Crystallite Size (101) (nm)	
	Particulate (%)	Film (%)	Particulate	Film
ZnO	74.39	26.49	25.09	5.69
TiO_2	80.50	24.59	56.95	48.66
TiO_2/ZnO	75.13	15.60	79.94 (TiO_2) 18.62 (ZnO)	39.35 (TiO_2) - (ZnO)

SEM-EDS Characterization

SEM-EDS analysis for the ZnO, TiO_2, and TiO_2/ZnO films were carried out to determine the morphology of all samples. Figure 3 shows the SEM images in 5000x and 20.000x magnification for all samples in layer and powder form, respectively. The TiO_2 layer easily identifiable as agglomerate particle clusters in the layer, but the sizes are cannot be recognized well. Since the TiO_2 particle is used as powder anatase, the change of particle size between powder and film form is observed. This result agrees with crystallite size calculation that explained previously. The ZnO film shows a defined morphology that is probably due to the small ZnO particulate size. Based on the previous results, the ZnO particle produced in the same route shows a nanosized less than 50 nm[21]. Fine fibers are visible on the surface of the ZnO film, which may result from the screen-printing deposition process. Meanwhile, the TiO_2/ZnO film has a denser morphology with a unique island surface. Other factors that can influence the morphology of the film include the composition, ingredients of the paste, and calcination temperature[17].

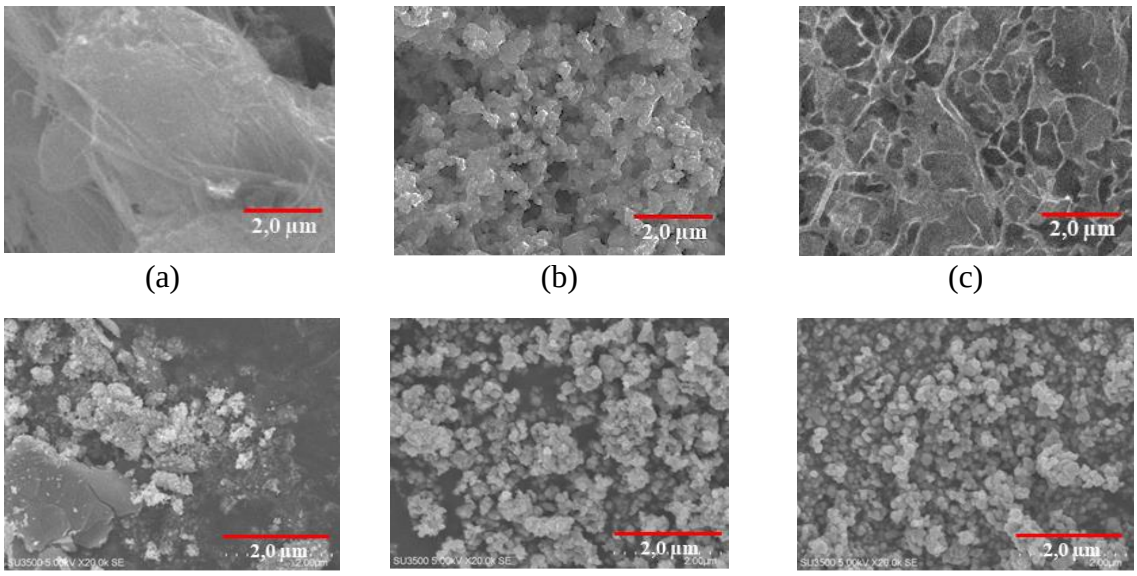

Figure 3. SEM of all samples in film (a-c) 5,000x and powder form 20,000x (d – f). (a) ZnO (b) TiO_2 (c) ZnO/TiO_2 (d) ZnO nanoparticle (e) TiO_2 particle (d) ZnO/TiO_2 particles (1:1)

Energy dispersive spectrum (EDS) analysis of ZnO/TiO_2 hetero-particle film determines the atomic and weight percentage of element composition which is tabulated in Table 2. The composition ratio between Zn and Ti atoms is approximately around 1:1. This result, provide

that the composition ratio is in accordance with the expectation. In the experimental step, the composition of ZnO-gel precursor was adjusted to obtain the same weight/atom with TiO_2 [1]. In fact, the weight percent of oxygen element inside the TiO_2/ZnO film is non-stochiometric, which is relate to the defect states such as zinc and titanium interstitial or oxygen vacancies [19].

Table 2. EDS results of TiO_2/ZnO film

Element	Weight%	Atomic%
O	44.19	73.08
Ti	29.45	16.26
Zn	26.37	10.67

Contact Angle Characterization

The surface characteristics that relate to wetting properties of the material can be observed using the water contact angle (CA) examination. This characterization method allows us to determine whether a sample is a hydrophilic or hydrophobic surface. If the contact angle is less than 90°, the sample surface is considered hydrophilic, whereas if higher than 90°, the surface is hydrophobic[22]. Wetting properties on material surfaces are determined by two factors: surface chemistry and surface topography[23]. On smooth surfaces, the wetting characteristic follows the young equation. Hence, the only determining factor is surface chemistry[24]. Adding certain surfactants can induce a chemical modification, which can increase or decrease the surface energy[23]. The CA measurement only provides for all sample films. The water droplet on the film surface was captured by the high-resolution camera (Canon G7X mark II). The high-resolution image allows us to observe and measure the angle between solid and liquid surfaces.

Based on SEM images, all sample films are identified as roughness and heterogeneous surfaces. CA measurement result shows a different wetting property between individual materials and their combination, as shown in Figure 5. ZnO has surfaces that tend to be hydrophobic ($\theta = 83.9°$), and the TiO_2 layer has hydrophobic surfaces ($\theta = 110.25°$). The TiO_2/ZnO hetero-particle layers have hydrophilic surfaces with $\theta = 30.9°$. Since all samples use the same solvent and surfactant, a different water contact angle estimated occurs by individual responses of each material to the triton-x100 as a surfactant. Triton-x 100 is a non-ionic surfactant with a hydrophilic head and hydrophobic end tail[25]. This surfactant dissolved the particle, leading them to attach and binds together. In fact, ZnO and TiO_2 are easily dissolved in polar solvents, which causes the hydrophilic head of the surfactant to attach. Since the calcination temperature occurred at 250 ℃, where the flash point of triton-x is at 251℃, the triton-x100 molecule is assumed to remain. This situation makes the surfaces of the ZnO and TiO_2 films tend to be/have hydrophobic surfaces. Different situations occur in TiO_2/ZnO hetero-particles. The mixing of ZnO-gel precursor (which is assumed as ZnOH) with TiO_2 anatase induces a change of the chemical surface of interfacial between TiO_2 and ZnO. TiO_2 has a positive charge in an acidic solution meanwhile, ZnOH is alkaline, which makes changes in acid to a neutral/alkaline environment and produces a different surface charge of TiO_2/ZnO hetero particle. The mixture makes the end tail (hydrophobic) of the surfactant attached to the TiO_2/ZnO surfaces, leading to hydrophilic characteristics. Moreover, since the powdered ZnO particle used was calcinated at 150℃ and easily dispersed in an organic solvent, the chemical reaction between the solvent and surfactant occurred, leading to the ZnO particle transformation to an amorphous structure.

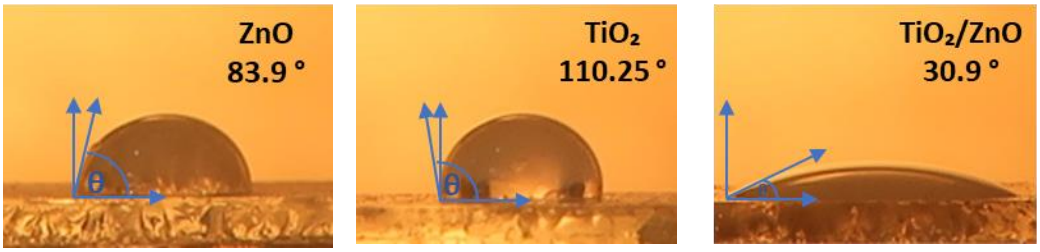

(a) (b) (c)

Figure 5. Contact angle measurement (a) ZnO (b) TiO_2 (c) TiO_2/ZnO

Photoluminescence Characterization

Defect sites of each sample can be observed through photoluminescence (PL) spectra in the visible spectrum (green emission). The PL characterization was performed within the wavelength range of 300 nm to 900 nm, involving an excitation wavelength of 315 nm. The different emission spectrum is observed between particulate and films form, as shown in Figure 6. Emission spectra in particulate form dominantly occur in the UV region that relates with near band emission (bandgap) rather than the visible region. The high intensity of UV emission is strongly correlated with a better crystallinity of the samples[26]. The PL spectra of all samples show blue emission in the visible region. Defect types at visible emission are observed by deconvolution of each PL spectrum. The ZnO and ZnO/TiO_2 hetero-particle film exhibit dominantly zinc vacancies and zinc interstitial as defects in 436,6 nm and 438,5 nm[27], while the TiO_2 and ZnO/TiO_2 films dominantly Ti vacancies (V_{Ti}^{x} and V_{Ti}') and also at 499,5 represent tri-valent Ti ions in interstitial sites ($T_{i}\cdots$)[28]. The TiO_2 film has the lowest peak, indicating the lower charge carrier recombination compared to the other samples.

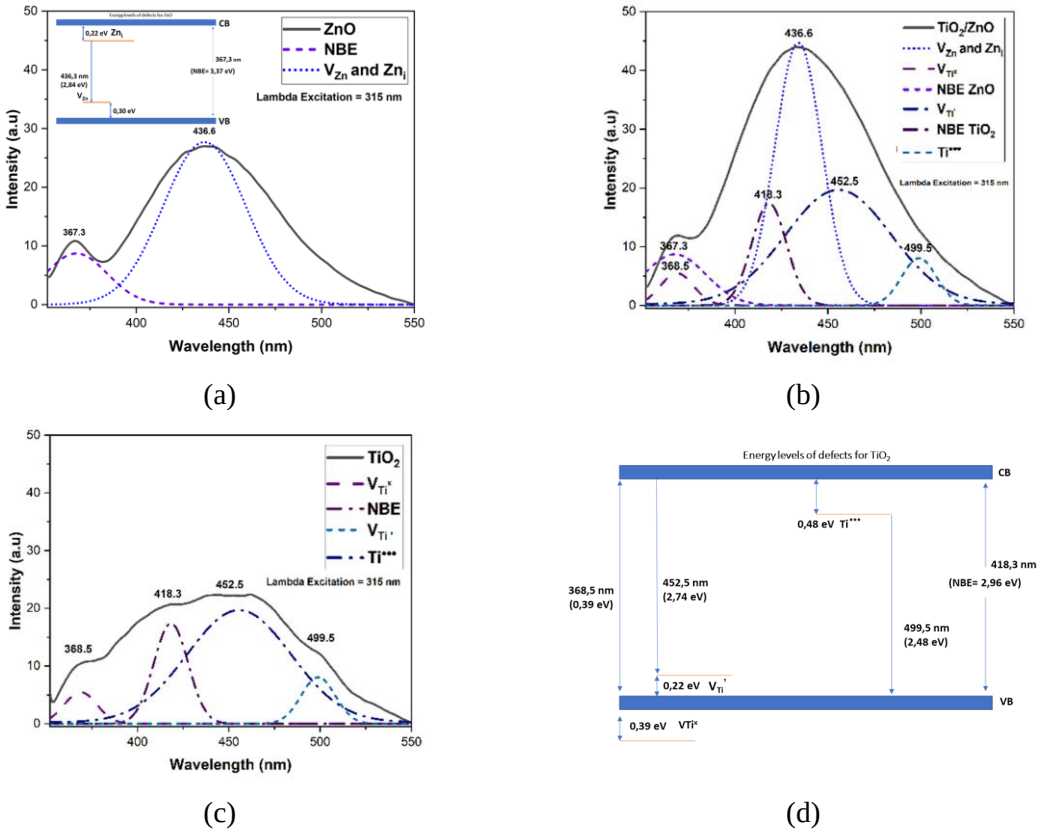

(a) (b)

(c) (d)

Figure 6. PL spectra of (a)ZnO, (b)TiO_2/ZnO, (c) TiO_2 films, and (d) energy levels of defect for TiO_2

Brunauer Emmett Teller (BET) Characterization

BET characterization was carried out to determine the specific surface area, pore radius, and pore volume of ZnO, TiO_2, and TiO_2/ZnO films and particulate, as tabulated in Table 3. The samples in films/film form have a larger specific surface area which is correlated by particle size. The particle size in the films form of all samples is estimated to be less than in the particulate form. ZnO is the largest specific surface area even in films and particulate form of 93.451 m^2/g and 28.395 m^2/g, respectively. Compared to individual TiO_2, the addition of ZnO in both of TiO_2/ZnO hetero-particle films and particulate hetero-particle increased the specific surface area from 67.86 to 79.875 m^2/g and 11.48 to 19.313 m^2/g, respectively. ZnO particle in films and particulate form was identified as a nanosized particle, increasing the specific surface area of TiO_2/ZnO hetero-particle. However, no significant differences were observed in the pore radius and volume of all sample films in the same group.

Table 3. BET Characterization Results

Sample	Specific Surface Area (m^2/g)	Pore Radius(nm)	Pore Volume (cm^3/g)
ZnO-f	93.451	1.7038	0.328
ZnO-p	28.395	2.077	8.37×10^{-3}
TiO_2-f	67.863	1.9133	0.292
TiO_2-p	11.480	5.025	2.744×10^{-3}
TiO_2/ZnO-f	79.875	1.7041	0.288
TiO_2/ZnO-p	19.313	2.086	8.61×10^{-3}

FTIR Fourier Transform Infrared (FTIR) Characterization

Fourier Transform Infrared (FTIR) characterization was performed to identify functional groups in the ZnO, TiO_2, and ZnO/TiO_2. The functional groups and bonds that exist in each material are described in Figure 7, which are compared with various references on FTIR studies of ZnO, TiO_2, and ZnO/TiO_2 materials [29-30]. The region of the infrared spectrum from 1500 to 400 cm^{-1} is analyzed as a fingerprint region of each molecule that is constructed in each sample[31]. In the fingerprint region from 750 – 400 cm^{-1} of FTIR spectra, confirm the formation of ZnO and TiO_2 bonds. The infra-red spectrum from 1500 – 750 cm^{-1} corresponds to the product of a reaction between ZnO precursors and TiO_2 anatase with the solvent and surfactant. The carbonyl bonds (1850 to 1650 cm^{-1}) and alkyl chain groups (3000 – 1800 cm^{-1}) are observed in film form originating from surfactant, indicating incomplete removal during calcination. In particulate form, the FTIR spectra both in the fingerprint region (1500 to 750 cm^{-1}) and carbonyl/alkyl groups are less observed. This difference suggests that the preparation methods induce a different chemical reaction and changes in functional groups due to the additives used and the calcination temperature during preparation. At wavenumbers around 3400 cm^{-1} is an O-H group, where the TiO_2 film has the lowest absorption group compared to other samples.

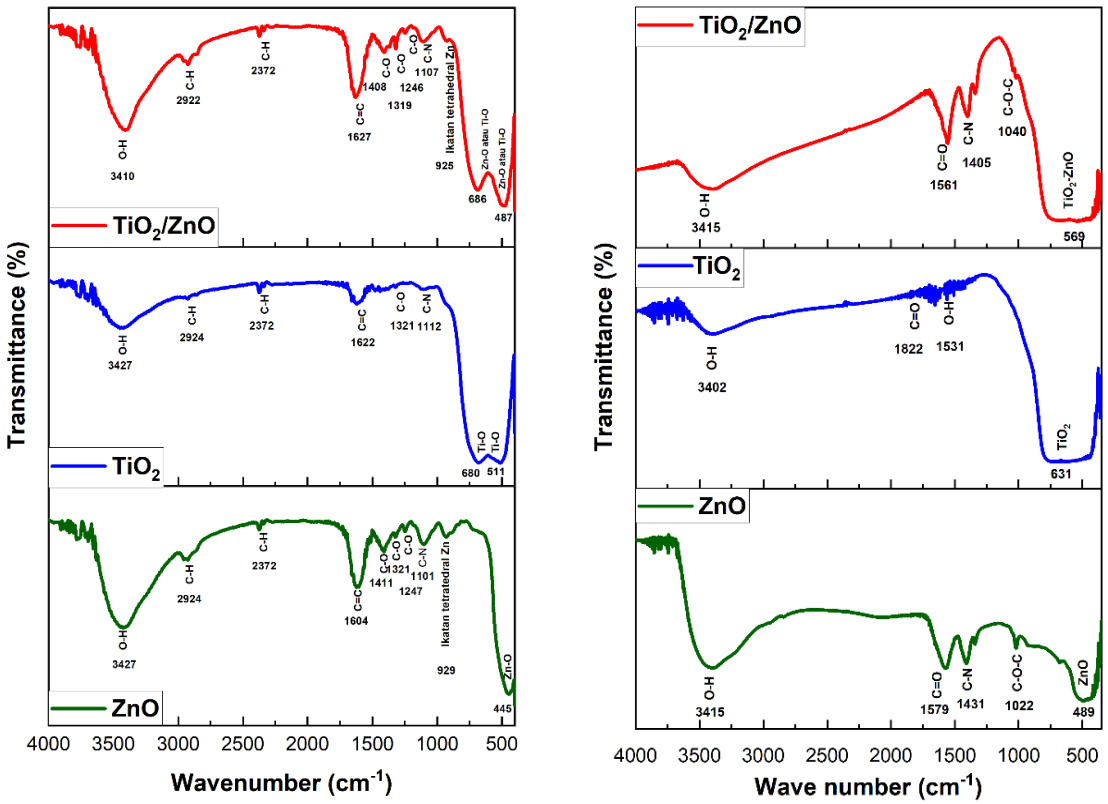

(a) (b)

Figure 7. Graph of FTIR spectrum measurements of ZnO, TiO_2, and TiO_2/ZnO (a) films (b) particulates

Photocatalytic Evaluation

Figure 8 shows MB degradation under UV-A irradiation incorporating all samples film and particulate catalysts. In this characterization, the MB concentration (C_0) is different for the samples film and particulate forms, which are 2.5 ppm and 5 ppm, respectively. The mechanism of MB degradation occurs through two kinds of processes. First is the adsorption of MB molecule by catalyst surface, which can be observed in 24-hour dark conditions before irradiation. Second is the photocatalytic mechanism that occurs during irradiation. Photocatalytic properties of all samples can be determined by calculating the degradation rate constant (k) using Equation(1). The efficiency (η) of MB degradation, including efficiency during adsorption (η_a) and photocatalytic processes (η_p) was calculated using Equation (2) and Equation (3), respectively[17]. For photocatalytic efficiency (η_p), the initial concentration (C_i) used in the calculation is after the catalysts have been immersed for 24 hours in dark conditions.

$$C(t) = C_0\, e^{-kt} \tag{1}$$

$$\eta_a = \frac{C_0 - C_i}{C_0} \cdot 100\% \tag{2}$$

$$\eta_p = \frac{C_i - C_t}{C_i} \cdot 100\% \tag{3}$$

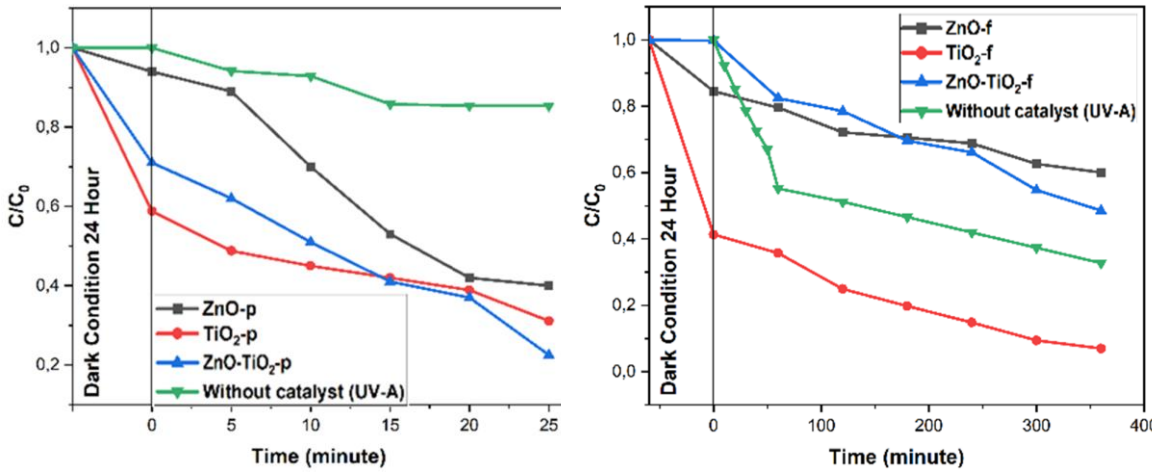

Figure 8. The photocatalyst degradation rate of MB (a) particulate (b) film

Table 4. Degradation of MB adsorption and photocatalytic mechanism under UV-A with/without catalyst samples

Sample	η	Efficiency in MB degradation mechanism				
		Adsorption (24-hours dark condition)	Photocatalytic			
		η_a	C_i/C_0	t (minutes)	η_p	k (/minutes)
UV-A	360' (68%)	0		25	15%	0.008
				360	68%	0.003
ZnO-f	360' (40%)	15%	0.85	360	14%	0.001
TiO_2-f	360' (93%)	60%	0.40	360	82%	0.005
TiO_2/ZnO-f	360' (52%)	1%	0.99	360	51%	0.002
ZnO-p	60%	10%	0.90	25	65%	0.039
TiO_2-p	69%	42%	0.58	25	46%	0.052
TiO_2/ZnO-p	78%	30%	0.70	25	69%	0.057

Since the concentration of MB is different, the observation is only appropriate to the trend of sample type in the different forms (group). Methylene blue (MB) can be degraded using the particulate group via adsorption and photocatalytic mechanism immediately at the first 25 minutes of irradiation, but not for the film group, as tabulated in Table 4. The results show different photocatalytic characteristics between film and particulate catalyst groups. In the particulate group, TiO_2/ZnO shows a better efficiency in MB degradation of 78% through adsorption and photocatalytic mechanism in 25 minutes of irradiation. Meanwhile, in the film group, better efficiency is obtained by TiO_2 film with 93% of MB in 360 minutes. Surprisingly,

the sample films show a reduction in photocatalytic performance in the ratio without a catalyst sample, especially with the ZnO incorporation. The UV-A irradiation can degrade 68% of MB in 360 minutes (k = 0.008/minutes). Meanwhile, ZnO and TiO_2/ZnO film only degraded 14% and 51% during the photocatalytic process (excluding the adsorption process). The total efficiency of MB degradation of ZnO and TiO_2/ZnO film is lower than UV-A irradiation by 40% (k = 0.001/minutes) and 61% (k = 0.002/minutes), respectively. Therefore, both samples

do not act as a catalyst but seem to work as UV-absorbance and prevent photons from degrading MB[32]. This unique property is estimated to be related to the crystal structure and morphology, as explained above[33]. ZnO's degree of crystallinity (DOC) is reduced significantly from 74.39% to 26.49%, and TiO_2/ZnO is reduced from 75.13% to 15.60%. This situation indicates a change in the chemical structure of ZnO during paste preparation since the sample powdered were prepared with the same route. This statement aligns with the morphology observation through SEM characterization

As shown in Table 4, TiO_2 film acts as catalyst material since MB was degraded 82% in 360 minutes of irradiation (93% MB degradation via adsorption and photocatalytic mechanisms). Based on the results from several characterizations above, the surfaces of TiO_2 films exhibit better MB adsorption than particulate forms, successfully maintain the catalyst property, and show hydrophobic surfaces. The hydrophobic characteristic of the catalyst gives other advantages to its catalytic activity. Catalysts with hydrophobic properties have been found to exhibit better catalytic activity due to the presence of an air films between the catalyst and the liquid. Sufficient oxygen in the air films can effectively trap electrons and form radicals that play a role in degrading pollutants, resulting in faster degradation and minimizing electron-hole recombination. The three-phase catalyst system (air-liquid-solid) shows higher photocatalytic activity compared to conventional two-phase (liquid-solid) systems[34].

CONCLUSION

The ZnO, TiO_2, and ZnO/TiO_2 films were successfully prepared using sol-gel and screen-printing techniques. The calcination of ZnO and TiO_2/ZnO hetero-particle was conducted at 150°C to facilitate the crystallization of the ZnO-wurtzite phase. Calcining at 250°C of all sample films was proposed to remove the other additive compounds, such as surfactants and solvents. The crystallinity of all the samples in film form was reduced, indicating that the other amorphous phase remains during paste preparation. The differences in surface morphology between the sample films provide different characteristics in wetting properties and catalytic performance. The TiO_2 film presented as hydrophobic ($\theta = 110°$), whereas the ZnO and ZnO/TiO_2 films demonstrated hydrophilic surfaces. Photoluminescence spectra of all sample films revealed dominant blue emissions associated with intrinsic defects such as interstitial and vacancies of zinc and titanium. Fourier Transform Infrared (FTIR) spectra confirmed the presence of appropriate chemical bonds for ZnO, TiO_2, and ZnO/TiO_2 hetero-particle films, validating the addition of the alkyl group and the successful formation of each material. The reduction in the catalytic performance of ZnO incorporated in the sample film is unexpected since ZnO gel phase were prepared with the same route and prepared first as particulate forms. In this case, the existence of ZnO seems to pretend to UV absorption and prevent dye degradation by UV-A rather than photocatalyst. A different structure, morphology, and effective surface area between film and particulate samples cause significant differences in photocatalytic performance. The synthesized ZnO, TiO_2, and ZnO/TiO_2 films provide valuable insights into their structural and surface properties, setting the stage for further exploration and potential applications in various fields. These results contribute to understanding the synthesis

and characterization of ZnO, TiO_2, and ZnO/TiO_2 films, providing a foundation for future research and advancements in the development of functional materials with enhanced properties.

REFERENCES

1 Ramadhika, L. N., Suryaningsih, S., & Aprilia, A. 2022. Photoactivity Enhancement of TiO_2 Nanoparticle-decorated ZnO as a Photocatalyst in Methylene Blue Degradation. *J. Phys. Conf. Ser, 2376*(1).

2 Petrov, V., Ignatieva,I., Volkova, M.G., Gulyaeva, I.A., & Pankov, I, V. 2023. Polycrystalline Transparent Al-Doped ZnO Thin Films for Photosensitivity and Optoelectronic Applications. *Nanomaterials, 13*(2348)

3 Chan, S.H.S., Wu, T.Y., Juan, J.C., & Teh, C.Y. Recent developments of metal oxide semiconductors as photocatalysts in advanced oxidation processes (AOPs) for treatment of dye waste-water. *J. Chem. Technol. Biotechnol. 86*(9), 1130-1158.

4 Upadhyay, G. K., Rajput, J. K., Pathak, T. K., Kumar, V., & Purohit, L. P. 2019. Synthesis of ZnO:TiO_2 nanocomposites for photocatalyst application in visible light. *Vacuum, 160*, 154–163.

5 Hellen, N., Park, H., & Kim, K. N. 2018. Characterization of ZnO/TiO_2 nanocomposites prepared via the sol-gel method. *J. Korean Ceram. Soc, 55*(2), 140–144

6 Amananti, W., & Susanto, H. 2016. Aktivitas Fotokatalis TiO_2 dan TiO_2/ZnO yang Dideposisikan diatas Subtrat Kaca Menggunakan Metode Sol-Gel Spray Coating. *PSEJ (Pancasakti Sci. Educ. Journal), 1*(1), 78–85.

7 Gayathri, P. V., Yesodharan, S., & Yesodharan, E. P. 2019. Microwave/Persulphate assisted ZnO mediated photocatalysis (MW/PS/UV/ZnO) as an efficient advanced oxidation process for the removal of RhB dye pollutant from water. *J. Environ. Chem. Eng, 7*(4**)**, 103122.

8 Das, A., Kumar, P. M., Bhagavathiachari, M., & Nair, R. G. 2020. Hierarchical ZnO-TiO_2 nanoheterojunction: A strategy driven approach to boost the photocatalytic performance through the synergy of improved surface area and interfacial charge transport. *Appl. Surf. Sci, 534*, 147321

9 Pei, L. Z., Wei, T., Lin, N.,& Yu, H. Y. 2016. Synthesis of zinc oxide and titanium dioxide composite nanorods and their photocatalytic properties. *Adv. Compos. Lett, 25*(1), 9–15.

10 Arabnezhad, M., Shafiee Afarani, M., & Jafari, A. 2019. Co-precipitation synthesis of ZnO–TiO_2 nanostructure composites for arsenic photodegradation from industrial wastewater. *Int. J. Environ. Sci. Technol. 16*(1), 463–468.

11 Wanghomode, J.V., Bhosale S.E., Shinde, T.B., Mohite, V.R., & Sapkal R.T. 2017. Synthesis of ZnO:TiO_2 Nanocomposite Thin Films by Spraypyrolysis. *Int. Res. J. of Science & Engineering, A1*(Special Issue), 55–58.

12 Ibrahim, Y., Isah, H.M., Abubakar, A., & Aminu, A.K. 2020. Comparative Studies on the Photocatalytic Degradation of Acridine Orange Using ZnO and ZnO/TiO_2 Synthesized Catalysts. *Nigerian Research Journal of Chemical Sciences, 8*(1), 328–338.

13 Habib, M. A., Shahadat, M. T., Bahadur, N. M., Ismail, I. M. I., & Mahmood, A. J. 2013. Synthesis and characterization of ZnO-TiO_2 nanocomposites and their application as photocatalysts. *International Nano Letters,3*(1), 1–8.

14 Ong, C. B., Ng, L. Y., & Mohammad, A. W. 2018. A review of ZnO nanoparticles as solar photocatalysts: Synthesis, mechanisms and applications. *Renew. Sustain. Energy Rev, 81*, 536–551.

15 Umehara, K., Yamada, T., Hijikata, T., Ichikawa, Y., & Katsube, F. 1997. Advanced ceramic substrate: Catalytic performance improvement by high geometric surface area and low heat capacity. *SAE Tech. Pap, 106*, 394–401.

16 Fosso-Kankeu, E., Pandey, S., & Ray, S. S. 2020. *Photocatalysts in Advanced Oxidation Processes for Wastewater Treatment*. Wiley Global Headquarters, USA.

17 ŞAHİN, B., & AYDIN, R. 2018. Enhancement Physical Performance of Nanostructured CuO Films via Surfactant TX-100. *Süleyman Demirel University Journal of Natural and Applied Sciences*, 1-8.

18 Ungár, T. 2004. Microstructural parameters from X-ray diffraction peak broadening. *Scr. Mater. 51*(8). 777-781

19 Shhamsuzan, Mashrai.A., Khanam, H., & Aljawfi, R.N. 2017. Biological synthesis of ZnO nanoparticles using C. albicans and studying their catalytic performance in the synthesis of steroidal pyrazolines. *Arab.J. Chem. 10.*

20 Darsono, T., Muqoyyanah, Sulhadi, Wahyuni, S., Marwoto, P., & Sugianto. 2021. Effect of Post-Annealing Treatment on the Morphological and Optical Properties of ZnO Thin Film Fabricated by Spraying Deposition Method. *Indones.J. Appl. Phys, 11*(1).
21 Aprilia, A., Mutiara, R., Afrilia, C.G., Bahtiar, A., Suryaningsih, S., & Safriani. L. 2021. Preliminary study of ZnO/GO composite preparation as photocatalyst material for degradation methylene blue under low UV-light irradiation. *Mater. Sci. Forum, 1028,* 319–325.
22 Rosales, A., & Esquivel, K. 2020. SiO_2@TiO_2 composite synthesis and its hydrophobic applications: A review. *Catalysts*. *10*, 1-17.
23 Ellinas, K., Dimitrakellis, P., Sarkiris, P., & Gogolides, E. 2021. A review of fabrication methods, properties and applications of superhydrophobic metals. *Processes*, 9, 1-29.
24 Akbari, R., & Antonini, C. 2021. Contact angle measurements: From existing methods to an open-source tool. *Adv. Colloid Interface Sci, 294,* 102470.
25 Farsang, E., Gaál, V., Horváth, O., Bárdos, E., & Horváth, K. 2019. Analysis of non-ionic surfactant Triton X-100 using hydrophilic interaction liquid chromatography and mass spectrometry. *Molecules*, *24*, 1-3.
26 Bousslama, W., Elhouichet, H., Gelloz, B., Sieber, B., Addad, A., Moreau, M., Férid, M.,& Koshida, N. 2012. Structural and luminescence properties of highly crystalline ZnO nanoparticles prepared by Sol-Gel method. *Jpn. J. Appl. Phys, 51*, 1-6.
27 Ching, K. L., Li, G., Ho, Y. L., & Kwok, H. S. 2016. The role of polarity and surface energy in the growth mechanism of ZnO from nanorods to nanotubes. *CrystEngComm*, 1-8.
28 Nowotny, J. 2008.Titanium dioxide-based semiconductors for solar-driven environmentally friendly applications: Impact of point defects on performance. *Energy Environ. Sci, 1,* 565–572.
29 Al-Taweel, S. S., & Saud, H. R. 2016. New route for synthesis of pure anatase TiO_2 nanoparticles via utrasound-assisted sol-gel method. *J. Chem. Pharm. Res, 8*(2), 620–626.
30 Rusman, E., Heryanto, H., Nurul Fahri, A., Tahir, D., & Mutmainna, I. 2021. Green Synthesis ZnO/TiO_2 for High Recyclability Rapid Sunlight Photodegradation Textile Dyes Applications. *ResearchSquare*.
31 Wade Textmap. 2023. *Organic chemistry*, LibreText.
32 Tsuzuki, T. He, R., Wang, J., Sun, L., & Wang, X. 2012. Reduction of the photocatalytic activity of ZnO nanoparticles for UV protection applications. *Int. J. Nanotechnol, 9,* 1017–1029.
33 Shaymardanov, Z.S., Rustamova, B.N., Jalolov, R.R., & Urolov S.Z. 2022. Influence of the nature of defects in ZnO nanocrystals synthesized by chemical bath deposition on photocatalytic activity. *Phys. B Condens Matter. 649*.
34 Liu, J., Ye, L., Wooh, S., Kappl, M. Steffen, W., & Butt, H. 2019. Optimizing Hydrophobicity and Photocatalytic Activity of PDMS-Coated Titanium Dioxide. *ACS Appl. Mater. Interfaces, 11,* 27422–27425.